



## Quantum chemical study of molecular structure, non-linear optical and vibrational properties of pyridine and pentachloropyridine

Satish Chand<sup>a</sup>, Shilendra K. Pathak<sup>a</sup>, Alok K. Sachan<sup>a</sup>, Ruchi Srivastava<sup>a</sup>, Vikas K. Shukla<sup>a</sup>, V. Narayan<sup>b</sup>, A. Kumar<sup>a</sup>, Onkar Prasad<sup>a</sup> and Leena Sinha<sup>a</sup>

<sup>a</sup>Department of Physics, University of Lucknow, Lucknow, India

<sup>b</sup>S. R. M. G. P. C., Lucknow, India

---

### ABSTRACT

A comprehensive investigation of the ground state structural, spectral and electronic properties of Pyridine and Pentachloropyridine (PCP) have been performed using B3LYP/6-311++G (d,p) level of theory. The complete vibrational assignment and analysis of the fundamental modes of both molecules were carried out using theoretical and experimental FTIR spectral data. The effect of substitution of electronegative chlorine atoms at the Pyridine ring, on the structural, vibrational and other properties has been analyzed and discussed. The frontier molecular orbitals analysis and molecular electrostatic potential surface (MESP) map have also been calculated to get a better insight of the properties of the title molecules. The mean polarizability of PCP is found to be 3.66 times more than Pyridine, whereas the dipole moment for Pyridine and PCP are calculated to be 2.3654 and 1.5262 Debye respectively.

**Keywords:** Optimized structure, HOMO-LUMO, MESP, Pyridine, Pentachloropyridine.

---

### INTRODUCTION

Pyridines and its derivatives are heterocyclic compounds that are the building blocks of a large number of biologically important molecules. The chemistry and applications of pyridine compounds have recently received much attention due to their efficacy as synthetic intermediates and biological importance [1,2]. The present communication deals with a comparative study of structural, vibrational and electronic properties of Pyridine and its derivative Pentachloropyridine (PCP). In order to obtain the complete description of molecular dynamics, vibrational wave number calculation along with normal mode analysis has been carried out at the DFT level of theory. A comprehensive investigation of geometric and electronic structure in ground state and first excited state, dipole moment, polarizability, first static hyperpolarizability along with molecular electrostatic potential surfaces may lead to the better understanding of structural and spectral characteristics of title compounds. The thermodynamic properties of compounds under investigation at different temperatures were also calculated.

#### 2.0 Theoretical and Experimental approach:

All theoretical calculations were performed with the Gaussian 09 program[3]. The ground-state geometry of Pyridine and PCP was optimized using the DFT-B3LYP theory [4,5] with the 6-311++G(d,p) basis set. IR spectra of both the compounds were calculated under the harmonic approximation at the same level of theory. The absence of imaginary wavenumber confirms that optimized structure of Pyridine and PCP correspond to minima on the potential energy surface. In general, DFT harmonic treatment overestimates vibrational wavenumbers owing to neglect of anharmonic corrections and incompleteness of basis set. These discrepancies are commonly corrected directly by scaling the calculated wavenumbers with an empirical uniform scaling factor of 0.983 up to 1700 cm<sup>-1</sup> and 0.958 for greater than 1700 cm<sup>-1</sup> [6,7]. GaussView5.0 [8] program has been used to get visual animation for

verification of the normal modes assignment. The experimental FT-IR spectrums of the title molecules were obtained from the website of NIST [9].

The DFT/B3LYP theory was also used to calculate the dipole moment ( $\mu$ ), mean polarizability  $\langle\alpha\rangle$ , anisotropy of polarizability ( $\Delta\alpha$ ) and the total first static hyperpolarizability ( $\beta$ ) [10,11]. As per Buckingham's definitions [12], the total dipole moment and the mean polarizability in the Cartesian frame are define as

$$\mu = (\mu_x^2 + \mu_y^2 + \mu_z^2)^{1/2} \quad ; \quad \langle\alpha\rangle = 1/3 [\alpha_{xx} + \alpha_{yy} + \alpha_{zz}],$$

$$\Delta\alpha = 2^{-1/2} [(\alpha_{xx} - \alpha_{yy})^2 + (\alpha_{yy} - \alpha_{xx})^2 + 6\alpha_{xx}^2 + 6\alpha_{xy}^2 + 6\alpha_{yz}^2]^{1/2}$$

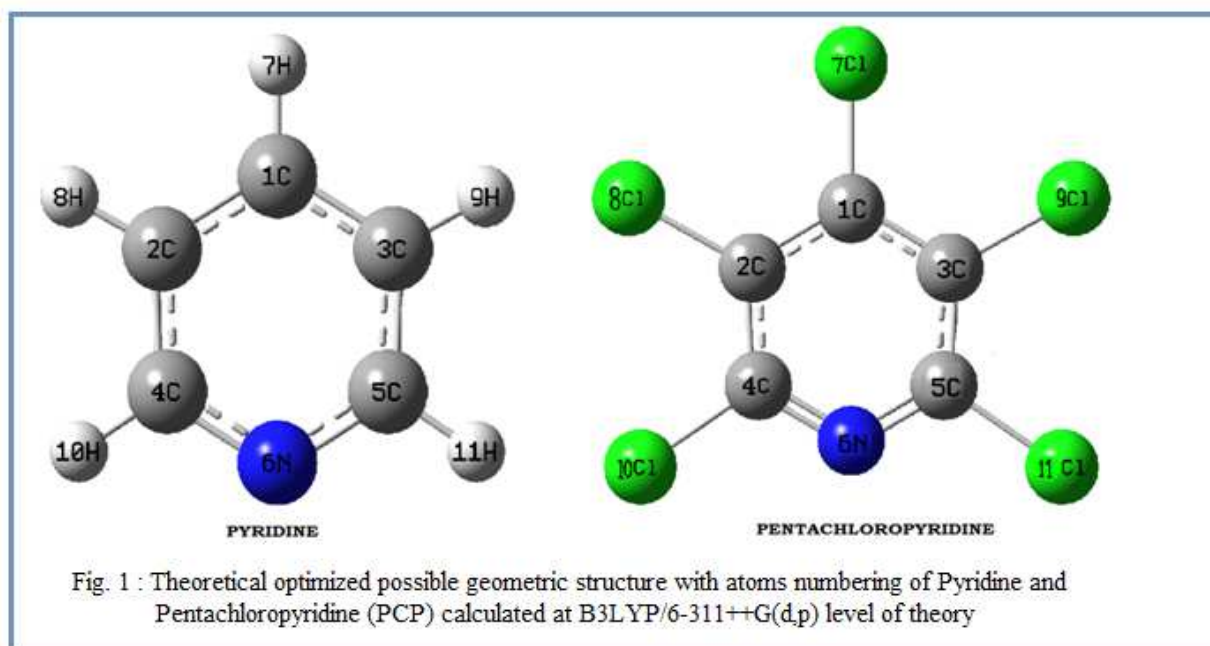
The total intrinsic hyperpolarizability  $\beta_{TOTAL}$  [11] is define as  $\beta_{TOTAL} = (\beta_x^2 + \beta_y^2 + \beta_z^2)^{1/2}$

Where,  $\beta_x = \beta_{xxx} + \beta_{xyy} + \beta_{xzz}$ ;  $\beta_y = \beta_{yyy} + \beta_{yzz} + \beta_{yxx}$ ;  $\beta_z = \beta_{zzz} + \beta_{zxx} + \beta_{zyy}$

The  $\beta$  components of Gaussian output are reported in atomic units and, therefore the calculated values are converted into e.s.u. units ( $\alpha$ ; 1 a.u. =  $0.1482 \times 10^{-24}$  e.s.u.,  $\beta$ ; 1 a.u. =  $8.3693 \times 10^{-33}$  e.s.u.)

## RESULTS AND DISCUSSION

### 3.1 Molecular Geometry Optimization



The structure of Pyridine and Pentachloropyridine (PCP) has been optimized to understand the variation in electronic and nonlinear properties on substitution of halogen group (chlorine) on pyridine. The molecular structure of the Pyridine and PCP optimized at DFT/B3LYP/6-311++G(d,p) level of theory is shown in **Fig. 1**. The ground state energy of the isolated molecule of pyridine (-248.3513 Hartree) is very large as compared to PCP (-2546.4423 Hartree), which shows that PCP is more stable than its parent pyridine molecule. The comparative optimized structural parameters such as bond lengths, bond angles and dihedral angles for both the molecules are collected in **Table 1**. The average C-C bond length in the Pyridine and PCP was found to be 1.393 Å and 1.402 Å respectively whereas mean C-N bond length in Pyridine and PCP were calculated to be 1.337 Å and 1.316 Å. The mean C-Cl bond length were found 1.734 Å in case of Pentachloropyridine (PCP). Bakiler et al. [13,14] calculated C-Cl bond length at 1.746 Å for 3-Cl-pyridine and 1.748 Å for 2-Cl-pyridine using force field calculations. The mean C-H bond length was calculated at 1.0852 Å in Pyridine. All interior C-C-C angle in Pyridine have greater value than PCP while trend was reversed in case of C-N-C angle which were found 117.3° and 120.1° respectively. All the dihedral angles were either 0° or 180° which shows that both the molecules are planner.

**Table 1: Optimized geometric parameters for Pyridine and Pentachloropyridine (PCP) computed at B3LYP/6-311++G(d,p) level of theory**

Parameters	Pyridine	PCP	Parameters	Pyridine	PCP
<b>Bond Length (Å<sup>0</sup>)</b>			<b>Bond Angle (in Degrees)</b>		
C1-C2	1.392	1.403	C3-C5-X11	120.3	120.8
C1-C3	1.392	1.403	N6-C5-X11	116.0	116.3
C1-X7	1.084	1.728	C4-N6-C5	117.3	120.1
C2-C4	1.394	1.401	<b>Dihedral Angles (in Deg.)</b>		
C2-X8	1.084	1.730	C3-C1-C2-C4	0.0	0.0
C3-C5	1.394	1.401	C3-C1-C2-X8	-180.0	-180.0
C3-X9	1.084	1.730	X7-C1-C2-C4	180.0	-180.0
C4-N6	1.337	1.316	X7-C1-C2-X8	0.0	0.0
C4-X10	1.087	1.742	C2-C1-C3-C5	0.0	0.0
C5-N6	1.337	1.316	C2-C1-C3-X9	-180.0	180.0
C5-X11	1.087	1.742	X7-C1-C3-C5	180.0	180.0
<b>Bond Angle (in Degrees)</b>			X7-C1-C3-X9	0.0	0.0
C2-C1-C3	118.5	119.6	C1-C2-C4-N6	0.0	0.0
C2-C1-X7	120.7	120.2	C1-C2-C4-X10	-180.0	-180.0
C3-C1-X7	120.7	120.2	X8-C2-C4-N6	180.0	180.0
C1-C2-C4	118.5	117.2	X8-C2-C4-X10	0.0	0.0
C1-C2-X8	121.3	121.2	C1-C3-C5-N6	0.0	0.0
C4-C2-X8	120.3	121.6	C1-C3-C5-X11	-180.0	180.0
C1-C3-C5	118.5	117.2	X9-C3-C5-N6	180.0	-180.0
C1-C3-X9	121.3	121.2	X9-C3-C5-X11	0.0	0.0
C5-C3-X9	120.3	121.6	C2-C4-N6-C5	0.0	0.0
C2-C4-N6	123.6	122.9	X10-C4-N6-C5	180.0	180.0
C2-C4-X10	120.3	120.8	C3-C5-N6-C4	0.0	0.0
N6-C4-X10	116.0	116.3	X11-C5-N6-C4	180.0	-180.0
C3-C5-N6	123.6	122.9			

*X = H and Cl for Pyridine and PCP respectively*

### 3.2 Electronic Properties

The most important orbitals in a molecule are the frontier molecular orbitals, termed as highest occupied molecular orbital (HOMO) and lowest unoccupied molecular orbital (LUMO). These orbitals determine the way how molecule interacts with other species. The frontier orbital gap helps to characterize the chemical reactivity and kinetic stability of the molecule. A molecule with a small frontier orbital gap is more polarizable and is generally associated with a high chemical reactivity and low kinetic stability so termed as soft molecule [15].

The 3D plots of frontier molecular orbitals shown in Fig. 2 envisage that HOMO is homogeneously spread over the entire molecule in Pyridine while in PCP it does not encompass the nitrogen atom and one chlorine atom. The LUMO is distributed uniformly in both molecules. The lower value of the frontier orbital gap in PCP (5.26323 eV) as compared to Pyridine (6.09018 eV) clearly shows that PCP is more polarizable and chemically reactive than Pyridine.

The molecular electrostatic potential surface (MESP), which is a method of mapping electrostatic potential onto the iso-electron density surface, simultaneously displays electrostatic potential (electron + nuclei) distribution, molecular shape, size and dipole moments and it provides a visual method to understand a relative polarity. The MESP plot of the title molecules is shown in Fig. 3. The prominent yellowish red region around the N atom in case of Pyridine makes it more electronegative as compared to PCP.

### 3.3 NLO Analysis

Nonlinear optical (NLO) effects arise from the interactions of electromagnetic fields in various media to produce new fields altered in phase, frequency, amplitude or other propagation characteristics from the incident fields [16]. NLO is at the forefront of current research because of its importance in providing the key functions of frequency shifting, optical modulation, optical switching, optical logic, and optical memory for emerging technologies in the areas such as telecommunications, signal processing, and optical interconnections [17-20]. Urea is one of the prototypical molecules used in the study of the NLO properties of molecular systems. Therefore it is used frequently as a threshold value for comparative purposes. The calculated values of dipole moment, mean polarizability, first static hyperpolarizability are given in Table-2. The calculated values of  $\mu$ ,  $\langle\alpha\rangle$  and  $\beta_{\text{TOTAL}}$  for the Pyridine/PCP were found 2.3654D/1.5262D, 61.117a.u./129.786 a.u. and  $0.115 \times 10^{-30}$  e.s.u./ $0.236 \times 10^{-30}$  e.s.u. by using B3LYP/6-311++G(d,p) basis set. The PCP has large  $\beta_{\text{TOTAL}}$  value greater than urea ( $0.1947 \times 10^{-30}$  e.s.u.), which indicates, PCP can be a good candidate of NLO material.

Table 2: Polarizability and first order hyperpolarizability data for Pyridine &amp; PCP at DFT -B3LYP/ 6-311++G(d,p) level of theory

Parameter	Pyridine	(PCP)	Parameters	Pyridine	(PCP)
<b>Dipole Moment (<math>\mu</math>)</b>			<b>First order static hyper-polarizability (<math>\beta</math>)</b>		
$\mu_x$	0.0000	0.0002	$\beta_{xxx}$	0.000	0.002
$\mu_y$	2.3654	1.5262	$\beta_{xxy}$	-1.931	1.815
$\mu_z$	0.0000	0.0001	$\beta_{xyy}$	0.003	0.001
$\mu_{\text{total}}$ (Debye)	2.3654	1.5262	$\beta_{yyy}$	16.537	24.570
<b>Polarizability (<math>\alpha</math>)</b>			$\beta_{xxz}$	0.001	-0.003
$\alpha_{xx}$	73.915	174.507	$\beta_{xyz}$	0.000	0.000
$\alpha_{xy}$	-1.749	0.000	$\beta_{yyz}$	0.000	-0.002
$\alpha_{yy}$	71.708	148.347	$\beta_{xzz}$	0.000	0.000
$\alpha_{xz}$	1.345	-0.001	$\beta_{yzz}$	-1.310	0.912
$\alpha_{yz}$	1.499	-0.001	$\beta_{zzz}$	0.000	0.001
$\alpha_{zz}$	37.730	66.503	$\beta_{\text{TOTAL}}$ (a.u.)	13.296	27.297
$\alpha_{\text{mean}}$ (a.u)	61.117	129.7857	$\beta_{\text{TOTAL}}$ (esu)	$0.115 \times 10^{-30}$	$0.236 \times 10^{-30}$
$\alpha_{\text{mean}}$ (esu)	$9.058 \times 10^{-24}$	$19.234 \times 10^{-24}$			

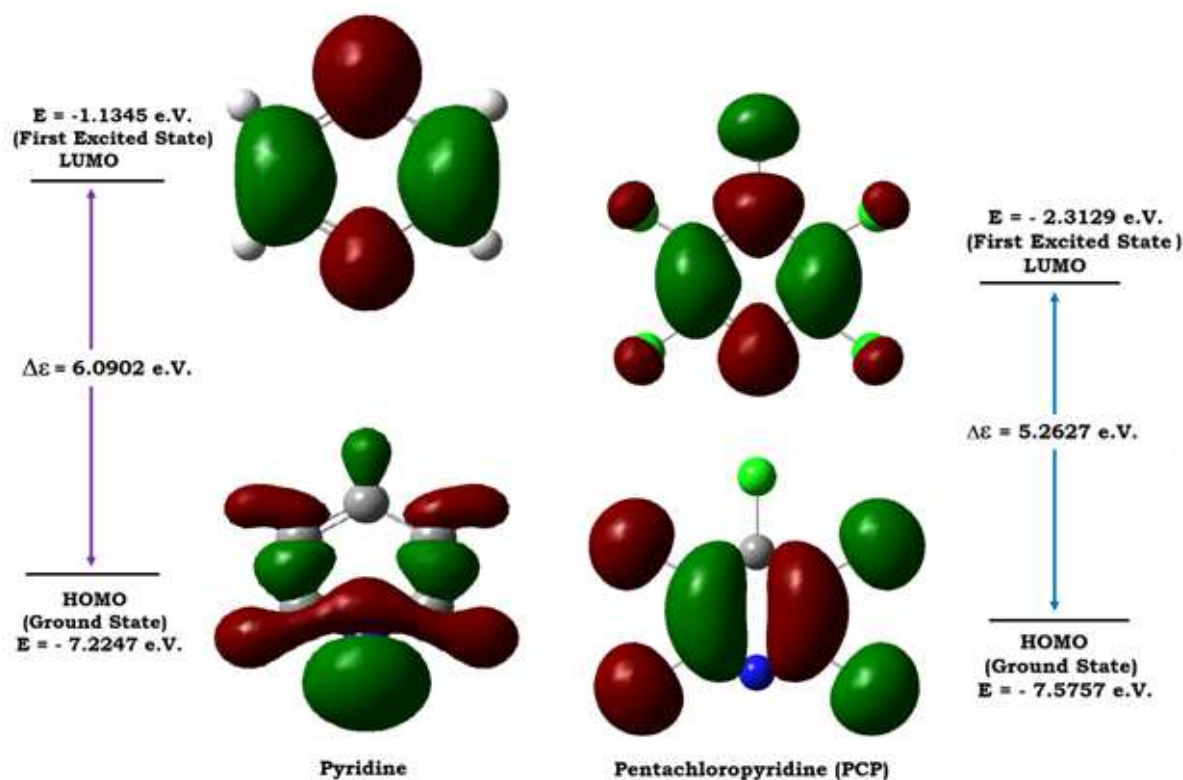


Fig. 2 : Patterns of frontier molecular orbitals (HOMO and LUMO) of Pyridine and Pentachloropyridine (PCP)

### 3.4 Vibrational Analysis

The experimental and calculated vibrational wavenumbers, their IR intensities and the detailed description of normal modes of vibration of both title compounds Pyridine and Pentachloropyridine (PCP) in terms of their contribution to the potential energy are given in Table 3 and 4 respectively. The experimental and theoretical IR spectrum of title molecules are shown in Fig. 4 and 5 respectively.

DFT based calculations provide not only the qualitative but also the quantitative understanding of energy distribution of each vibrational mode on the basis of potential energy distribution (PED) and lead to an additional interpretation of the vibrational spectroscopic data as demonstrated in studies conducted by various groups [21-24]. For normal coordinate analysis of the pyridine and pentachloropyridine, the complete set of 38 standard internal coordinates have been defined (Table 5) and using these internal coordinates, a non redundant set of 27 (i.e.  $3n-6$ ) local symmetry coordinates (Table 6) are constructed on the basis of recommendations of the G. Fogarasi et.al. [25-26]. The theoretical vibrational assignment of the title compounds using percentage potential energy distribution (PED) have been done with the MOLVIB program (version V7.0-G77) written by T. Sundius [27-29]

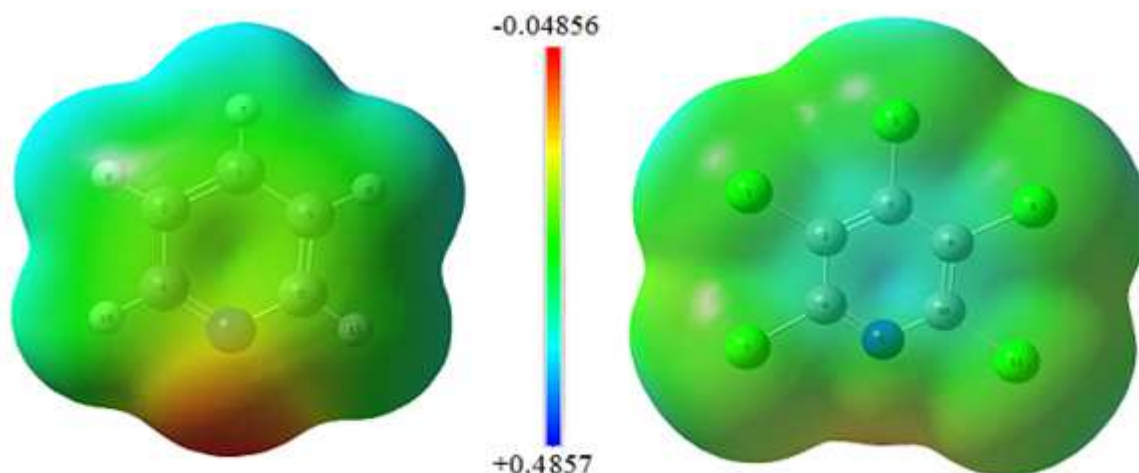


Fig. 3 : 3D MESP surface of Pyridine and Pentachloropyridine (PCP)

Both the title molecules consist of 11 atoms, hence undergoes 27 normal modes of vibrations. The hetero aromatic structure shows the presence of C–H stretching vibration in the region  $3100\text{--}3000\text{cm}^{-1}$  which is the characteristic region for the identification of C–H stretching vibration [30]. The absorption bands in experimental FTIR spectrum of the pyridine near  $3000\text{ cm}^{-1}$  are due the C–H stretching vibrations of aromatic ring and theoretically assigned at  $3060, 3052, 3037, 3017$  and  $3015\text{ cm}^{-1}$ . The vibrations involving C–H in-plane and out of plane bending modes are found throughout the region at  $1590\text{--}1058\text{ cm}^{-1}$  and  $989\text{--}703\text{ cm}^{-1}$  respectively which are good agreement with the medium intensity bands at  $1443$  and  $835\text{ cm}^{-1}$  respectively in FTIR spectra of pyridine.

Presence of heavy halogen atoms on the periphery of molecule causes mixing of vibrations belonging to the bond between the ring and the halogen atoms [31]. The absorption bands corresponding to C–Cl stretching vibrations in FTIR spectrum of the PCP compound are assigned as intense bands at  $820$  and  $672\text{ cm}^{-1}$  while the calculated wavenumbers for these stretching vibrations are in the region at  $867\text{--}324\text{ cm}^{-1}$ . The scaled wavenumbers corresponding to dominant C–Cl in plane and out of plane bending modes are  $571, 221, 214, 211, 199$  and  $619, 568, 359, 278, 146\text{ cm}^{-1}$  respectively.

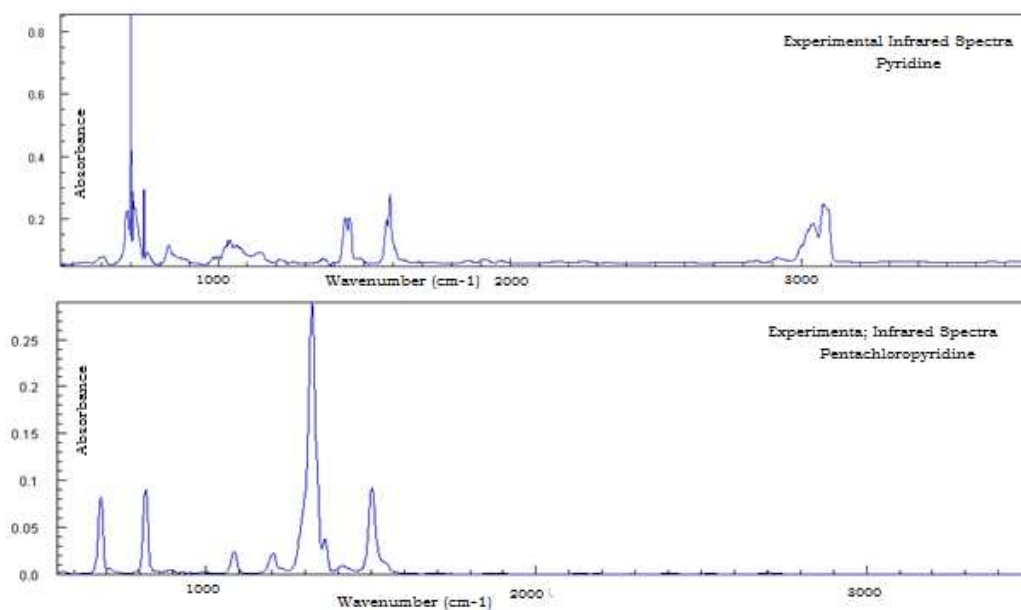


Fig. 4 : Experimental FT-IR spectra of Pyridine and Pentachloropyridine (PCP)

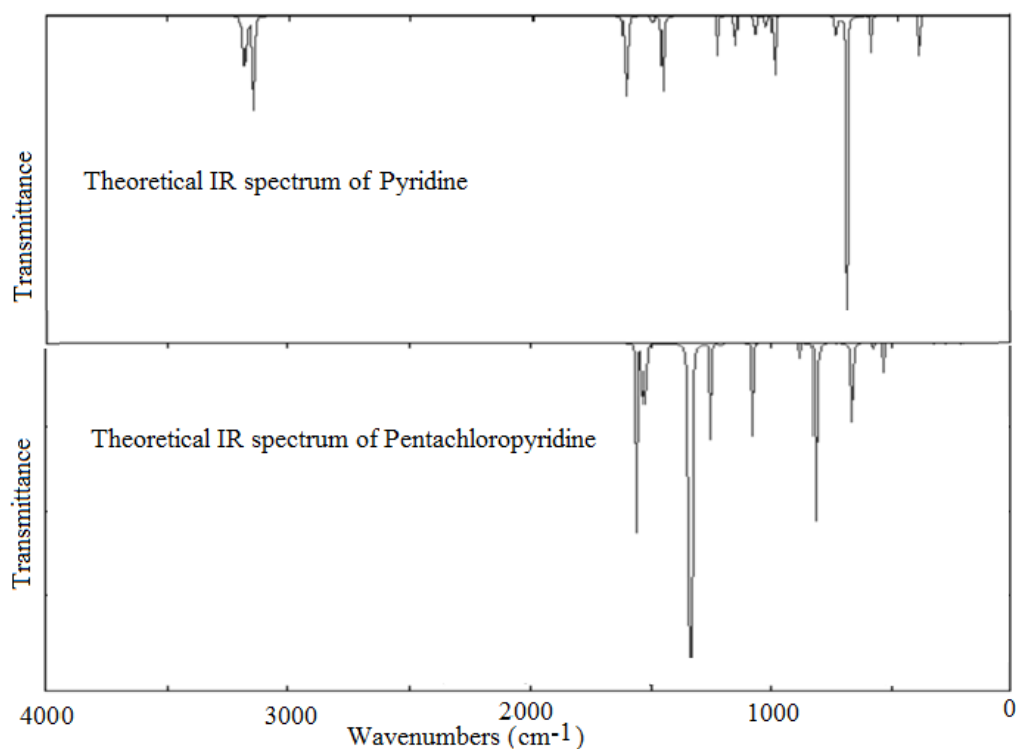


Fig. 5 : Theoretically calculated FT-IR spectra of Pyridine and Pentachloropyridine (PCP) at B3LYP/6-311++G (d,p) level of theory

Table 3: Comparison of experimental infrared wave numbers ( $\text{cm}^{-1}$ ) with calculated unsealed and scaled harmonic frequencies ( $\text{cm}^{-1}$ ) and infrared intensities along with their assignments

S. No.	Calculated Wave no.		Exp. W. no. FTIR	IR Inten.	Assignment of dominant modes with % (PED)
	Unsc.	Sca.			
1	3194	3060		6.89	$\nu\text{C-H}$ (96)
2	3186	3052	3062 m	25.03	$\nu\text{C-H}$ (96)
3	3170	3037	3028 w	4.98	$\nu\text{C-H}$ (92)
4	3149	3017		4.10	$\nu\text{C-H}$ (90)
5	3147	3015	3015 m	28.09	$\nu\text{C-H}$ (96)
6	1623	1595	1597 m	23.87	$\nu\text{C-C}$ (58) + $\delta R_{\text{assy1}}$ (9)
7	1617	1590		10.17	$\nu\text{C-C}$ (46) + $\beta\text{C-H}$ (12) + $\nu\text{C-N}$ (22) + $\delta R_{\text{assy2}}$ (10)
8	1510	1484		2.47	$\beta\text{C-H}$ (57) + $\nu\text{C-N}$ (22)
9	1470	1445		26.92	$\beta\text{C-H}$ (54) + $\nu\text{C-C}$ (42)
10	1384	1360	1343 w	0.05	$\beta\text{C-H}$ (98)
11	1284	1262		0.03	$\nu\text{C-N}$ (46) + $\nu\text{C-C}$ (35) + Kekule Mode
12	1241	1220		4.69	$\beta\text{C-H}$ (66) + $\nu\text{C-N}$ (21)
13	1170	1150		2.45	$\beta\text{C-H}$ (73) + $\nu\text{C-C}$ (20)
14	1093	1074		5.22	$\beta\text{C-H}$ (36) + $\delta R_{\text{trig}}$ (17) + $\nu\text{C-C}$ (24) + $\nu\text{C-N}$ (10)
15	1076	1058		0.00	$\nu\text{C-C}$ (46) + $\beta\text{C-H}$ (28)
16	1047	1029	1337 m	6.28	$\delta R_{\text{trig}}$ (51) + $\nu\text{C-C}$ (41)
17	1010	993		4.79	$\delta R_{\text{trig}}$ (41) + $\nu\text{C-N}$ (28) + $\nu\text{C-C}$ (16)
18	1006	989		0.00	$\rho\text{C-H}$ (79) + $\tau R_{\text{puck}}$ (12)
19	997	980		0.00	$\rho\text{C-H}$ (92) + $\tau R_{\text{assy2}}$ (8)
20	955	938		0.02	$\rho\text{C-H}$ (88) + $\tau R_{\text{puck}}$ (7)
21	892	877	835 w	0.00	$\rho\text{C-H}$ (99)
22	758	745	740 m	11.71	$\tau R_{\text{puck}}$ (62) + $\rho\text{C-H}$ (38)
23	715	703	708 s	67.28	$\tau R_{\text{puck}}$ (38) + $\rho\text{C-H}$ (57)
24	669	658		0.30	$\delta R_{\text{assy2}}$ (88)
25	617	606	595 m	3.61	$\delta R_{\text{assy1}}$ (89)
26	418	411		4.06	$\tau R_{\text{assy2}}$ (84)
27	381	374		0.00	$\tau R_{\text{assy2}}$ (86)

$\nu$ -Stretching,  $\delta$ -Deformation,  $\beta$ -In-plane bending,  $\rho$ -Rocking,  $\delta R$ -Ring deformation ( $R_{\text{trig}}$ -Trigonal Ring deformation,  $R_{\text{assy1}}$ -asymmetric deformation type-I,  $R_{\text{assy2}}$ -asymmetric deformation type-II);  $\tau R$  - Ring Torsion ( $R_{\text{puck}}$ -RingPuckring,  $R_{\text{assy1}}$ -asymmetric torsion type-I,  $R_{\text{assy2}}$ -asymmetric torsion type-II)

**Table 4: Comparison of experimental infrared wave numbers ( $\text{cm}^{-1}$ ) with calculated unscaled and scaled harmonic frequencies ( $\text{cm}^{-1}$ ) and infrared intensities along with their assignments for PCP**

S. No.	Calculated Wave no.		Exp. W. no. FTIR	IR Intensity	Assignment of dominant modes in order of decreasing potential energy distribution (PED)
	Unsc.	Scal.			
1	1556	1530	1538 w	63.15	$\nu\text{C-N (46)} + \nu\text{C-C (34)} + \delta\text{R}_{\text{assy-2}}(11)$
2	1527	1501	1508 m	101.83	$\nu\text{C-C (58)} + \delta\text{R}_{\text{assy-1}}(10) + \nu\text{C-N (16)}$
3	1344	1321	1310 s	126.13	$\nu\text{C-C (47)} + \nu\text{C-N (28)}$
4	1342	1319	1290 m	414.28	$\nu\text{C-C (48)} + \nu\text{C-N (24)}$
5	1257	1236	1205 w	38.14	$\nu\text{C-C (72)} + \nu\text{C-N (22)}$ Kekule Mode
6	1215	1194		3.85	$\nu\text{C-C(38)} + \nu\text{C-N (24)}$ RBM
7	1081	1063	1095 w	36.66	$\delta\text{R}_{\text{trig}}(68)$
8	882	867		3.58	$\nu\text{C-Cl (56)} + \delta\text{R}_{\text{assy2}}(39)$
9	816	802	820 m	94.54	$\nu\text{C-Cl (61)} + \delta\text{R}_{\text{assy1}}(32)$
10	739	726		0.15	$\tau\text{R}_{\text{puck}}(54) + \rho\text{C-Cl (46)}$
11	670	659	672 m	98.96	$\nu\text{C-Cl (62)} + \rho\text{C-Cl (18)}$
12	630	619		0.00	$\rho\text{C-Cl (72)} + \tau\text{R}_{\text{assy2}}(28)$
13	581	571		2.60	$\beta\text{C-Cl (93)}$
14	578	568		1.36	$\rho\text{C-Cl (51)} + \tau\text{R}_{\text{assy1}}(40)$
15	538	529		9.03	$\nu\text{C-Cl (46)} + \delta\text{R}_{\text{assy1}}(18) + \delta\text{R}_{\text{trig}}(8)$
16	380	373		0.21	$\nu\text{C-Cl (71)} + \delta\text{R}_{\text{trig}}(13)$
17	365	359		0.00	$\rho\text{C-Cl (98)}$
18	346	340		0.10	$\nu\text{C-Cl (60)} + \delta\text{R}_{\text{assy1}}(19)$
19	330	324		0.42	$\delta\text{R}_{\text{assy2}}(52) + \nu\text{C-Cl (22)}$
20	283	278		0.74	$\rho\text{C-Cl (77)} + \tau\text{R}_{\text{assy1}}(18)$
21	225	221		0.00	$\beta\text{C-Cl (93)}$
22	218	214		0.08	$\beta\text{C-Cl (90)}$
23	215	211		0.36	$\beta\text{C-Cl (87)}$
24	203	199		0.09	$\beta\text{C-Cl (80)} + \delta\text{R}_{\text{assy1}}(7)$
25	148	146		0.00	$\rho\text{C-Cl (87)} + \tau\text{R}_{\text{puck}}(7)$
26	79	78		0.02	$\tau\text{R}_{\text{assy1}}(61) + \tau\text{R}_{\text{puck}}(25)$
27	57	56		0.00	$\tau\text{R}_{\text{assy2}}(98)$

$\nu$ -Stretching,  $\delta$ -Deformation,  $\beta$ -In-plane bending,  $\rho$ -Rocking,  $\delta\text{R}$ -Ring deformation ( $\text{R}_{\text{trig}}$ -Trigonal Ring deformation,  $\text{R}_{\text{assy1}}$ -asymmetric deformation type-I,  $\text{R}_{\text{assy2}}$ -asymmetric deformation type-II);  $\tau\text{R}$  - Ring Torsion ( $\text{R}_{\text{puck}}$ -RingPuckring,  $\text{R}_{\text{assy1}}$ -asymmetric torsion type-I,  $\text{R}_{\text{assy2}}$ -asymmetric torsion type-II)

**Table 5 : Definition of internal coordinates of Pyridine and Pentachloropyridine with B3LYP/6-311++G(d,p)**

No. (i)	Symbol	Type	Definition
Stretching			
1-4	$r_i$	C-C	C1-C2, C2-C4, C5-C3, C3-C1
5-9	$r_i$	C-X	C4-X10, C2-X8, C1-X7, C3-X9, C5-X11
10-11	$r_i$	C-N	C4-N6, C5-N6
In-plane bending			
12-14	$\alpha_i$	C-C-C	C4-C2-C1, C2-C1-C3, C1-C3-C5
15-16	$\alpha_i$	C-C-N	C2-C4-N6, C3-C5-N6
17	$\alpha_i$	C-N-C	C4-N6-C5
18-25	$\alpha_i$	C-C-X	C3-C5-X11, C5-C3-X9, C1-C3-X9, C3-C1-X7, C2-C1-X7, C1-C2-X8, C4-C2-X8, C2-C4-X10
26-27	$\alpha_i$	N-C-X	N6-C4-X10, N6-C5-X11
Out-of-plane bending			
28-30	$\phi_i$	X-C	X9-C3-C1-C5, X7-C1-C3-C2, X8-C2-C1-C4
31-32	$\phi_i$	X-C	X10-C4-C2-N6, X11-C5-C3-N6
Torsion			
33-34	$T_i$	$\tau$ Ring	C4-C2-C1-C3, C2-C1-C3-C5
35-38	$T_i$	$\tau$ Ring	C1-C3-C5-N6, C3-C5-N6-C4, C5-N6-C4-C2, N6-C4-C2-C1

$X = \text{H and Cl for Pyridine and PCP respectively}$

The carbon-carbon stretching modes of the pyridine are expected in the range from 1650 to 1100  $\text{cm}^{-1}$  [32]. In this study the C-C stretching vibrations in pyridine are found to be in the region at 1595-1058  $\text{cm}^{-1}$  while in case of PCP these vibrations lie in the range at 1501-1194  $\text{cm}^{-1}$ . The experimental absorption band observed at 1597  $\text{cm}^{-1}$  in FT-IR spectrum of Pyridine and at 1508, 1310 and 1205  $\text{cm}^{-1}$  in that of PCP are assigned as carbon-carbon stretching vibrations of the ring. The interesting ring stretching Kekule mode is assigned at 1262 and 1236  $\text{cm}^{-1}$  for pyridine and PCP respectively. The very small variation in the wavenumber corresponding to Kekule mode shows insensitive nature of this mode for substitution. Identification of C-N vibration is very difficult task since mixing of several vibrations is possible in this region. In the present study the dominant C-N stretching bands are assigned at 1590 and 1262  $\text{cm}^{-1}$  in pyridine and at 1530, 1501 and 1194  $\text{cm}^{-1}$  in PCP, mixed with C-C stretching vibrations. The torsional

modes are generally found at lower wavenumber range. The remainder of the observed and calculated wavenumbers and their assignments for title molecules are shown in Table 3 and 4.

**Table 6: Definition of local symmetry coordinates of Pyridine & Pentachloropyridine (PCP)**

No. (i)	Symbol	Definition
1-4	v (C-C) Ring	$r_1, r_2, r_3, r_4$
5-9	v (C-X) Ring	$r_5, r_6, r_7, r_8, r_9$
10-11	v (C-N) Ring	$r_{10}, r_{11}$
12-14	$\beta$ C-X	$(\alpha_{24}-\alpha_{23})/\sqrt{2}, (\alpha_{22}-\alpha_{21})/\sqrt{2}, (\alpha_{20}-\alpha_{19})/\sqrt{2}$
15-16	$\beta$ C-X	$(\alpha_{26}-\alpha_{25})/\sqrt{2}, (\alpha_{18}-\alpha_{27})/\sqrt{2}$
17-21	$\rho$ C-X	$\phi_{28}, \phi_{29}, \phi_{30}, \phi_{31}, \phi_{32}$
22	$\delta R_{tri}$	$(\alpha_{13} - \alpha_{14} + \alpha_{16} - \alpha_{17} + \alpha_{15} - \alpha_{12})/\sqrt{6}$
23	$\delta R_{assy1}$	$(2\alpha_{13} - \alpha_{14} - \alpha_{16} + 2\alpha_{17} - \alpha_{15} - \alpha_{12})/\sqrt{12}$
24	$\delta R_{assy2}$	$(\alpha_{14} - \alpha_{16} + \alpha_{15} - \alpha_{12})/2$
25	$\tau R_{Puck}$	$(T_{34} - T_{35} + T_{36} - T_{37} + T_{38} - T_{33})/\sqrt{6}$
26	$\tau R_{assy1}$	$(T_{34} - T_{36} + T_{37} - T_{33})/2$
27	$\tau R_{assy2}$	$(-T_{34} + 2T_{35} - T_{36} - T_{37} + 2T_{38} - T_{33})/\sqrt{12}$

*X = H and Cl for Pyridine and PCP respectively*

### 3.5 Thermo dynamical Properties

The values of some thermodynamic parameter (such as zero-point vibrational energy, thermal energy, specific heat capacity, rotational constant and entropy) at standard temperature (298.15 K) for Pyridine and Pentachloropyridine (PCP) computed at DFT/B3LYP with 6-311G++(d,p) methods are listed in Table 7. On the basis of vibrational analysis, the standard statistical thermodynamic functions: heat capacity ( $C_{p,m}^0$ ), entropy ( $S_m^0$ ), and enthalpy change ( $\Delta H_m^0$ ) for the pyridine and pentachloropyridine were obtained from the theoretical harmonic frequencies and listed in Table 8.

**Table 7: The calculated thermo dynamical parameters of Pyridine and PCP at 298.15 K in ground state**

Parameter	Pyridine	Pentachloropyridine (PCP)
SCF Energy (in a.u.)	-248.3513	-2546.4423
$\epsilon_{HOMO}$ (in a.u. / e.V.)	-0.2655 a.u. / -7.2247 e.V.	-0.2784 a.u. / -7.5757 e.V.
$\epsilon_{LUMO}$ (in a.u. / e.V.)	-0.0417 a.u. / -1.1345 e.V.	-0.0850 a.u. / -2.3129 e.V.
$\epsilon_{HOMO-LUMO}$ (in a.u. / e.V.)	0.2238 a.u. / 6.0902 e.V.	0.1934 a.u. / 5.2626 e.V.
Zero Point Vibrational Energy (kcal/mol)	55.43493	25.16637
	6.05015	0.68680
Rotational Constants (GHz)	5.82898	0.47808
	2.96875	0.28187
Specific Heat ( $C_v$ ) (cal mol <sup>-1</sup> K <sup>-1</sup> )	16.216	35.166
Entropy (S) (cal mol <sup>-1</sup> K <sup>-1</sup> )	68.698	103.307

**Table 8 : Thermodynamic properties at different temperature for Pyridine and Pentachloropyridine (PCP)**

T (K)	Pyridine			Pentachloropyridine (PCP)		
	$C_{p,m}^0$ (cal mol <sup>-1</sup> K <sup>-1</sup> )	$S_m^0$ (cal mol <sup>-1</sup> K <sup>-1</sup> )	$\Delta H_m^0$ (kcal mol <sup>-1</sup> )	$C_{p,m}^0$ (cal mol <sup>-1</sup> K <sup>-1</sup> )	$S_m^0$ (cal mol <sup>-1</sup> K <sup>-1</sup> )	$\Delta H_m^0$ (kcal mol <sup>-1</sup> )
100	6.438	55.96	0.803	16.808	73.384	1.244
200	10.180	62.759	1.805	27.677	89.989	3.702
298.15	16.698	68.698	3.285	35.166	103.307	7.001
400	22.810	74.982	5.479	40.916	115.07	11.092
500	28.399	81.136	8.247	45.108	125.117	15.602
600	32.929	87.091	11.52	48.209	133.992	20.475
700	36.580	92.758	15.201	50.505	141.911	25.615

From Table 8, it can be observed that these thermodynamic functions are increasing with temperature ranging from 100 to 700K due to the fact that the molecular vibrational intensities increase with temperature [33,34]. The correlation equations among heat capacities, entropies, enthalpy change and temperatures were fitted by quadratic, linear and quadratic formulas and the corresponding fitting factors ( $R^2$ ) for these thermodynamic properties in case of pyridine are 0.99473, 0.99992, 0.99991 and in case of PCP are 0.99779, 0.99958, 0.99969 respectively. The corresponding fitting equations are as follows and the correlation graphics of these are shown in Fig. 6 and 7.



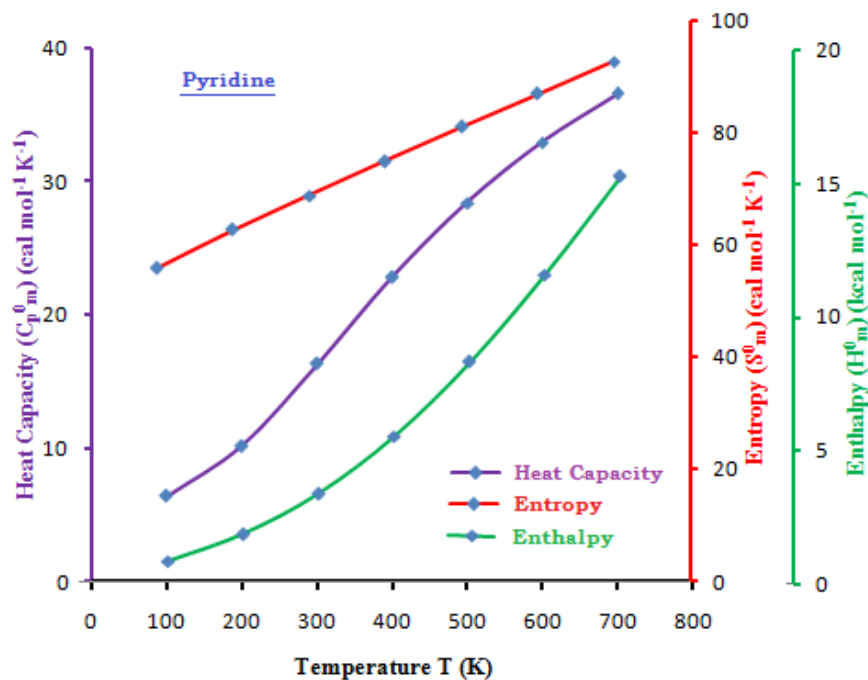


Fig. 6 : Correlation graph of Heat Capacity, Entropy and Enthalpy Vs temperature for Pyridine.

Pyridine:

$$C_{p,m}^0 = -0.66757 + 0.06272 T - 1.23381 \times 10^{-5} T^2 \quad (R^2 = 0.99473)$$

$$S_m^0 = 49.41929 + 0.06709T - 0.73560 \times 10^{-5} T^2 \quad (R^2 = 0.99992)$$

$$H_m^0 = 0.31843 + 0.00183 T + 2.78679 \times 10^{-5} T^2 \quad (R^2 = 0.99991)$$

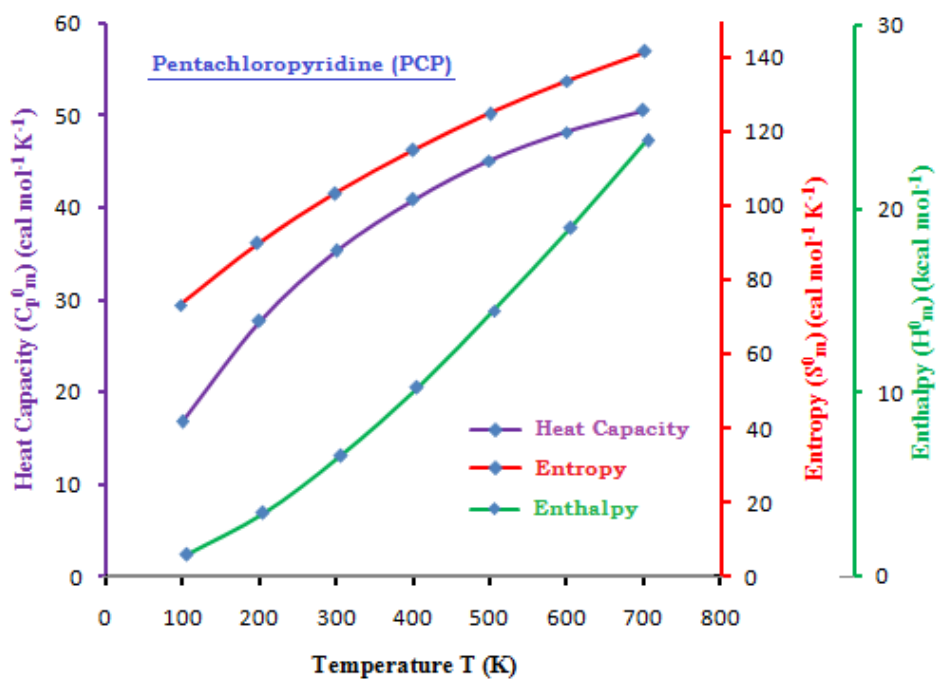


Fig. 7 : Correlation graph of heat capacity, entropy and enthalpy versus temperature for Pentachloropyridine (PCP).

Pentachloropyridine (PCP) :

$$C_{p,m}^0 = 6.32157 + 0.11931 T - 8.12869 \times 10^{-5} T^2 \quad (R^2 = 0.99779)$$

$$S_m^0 = 56.86657 + 0.17900 T - 8.30560 \times 10^{-5} T^2 \quad (R^2 = 0.99958)$$

$$H_m^0 = -1.21129 + 0.02027 T + 2.60881 \times 10^{-5} T^2 \quad (R^2 = 0.99969)$$

All the thermodynamic data supplied are helpful information for further study of pyridine and pentachloropyridine. These can be used to compute the other thermodynamic energies according to the relationships of thermodynamic functions and estimate directions of chemical reactions according to the second law of thermodynamics in thermo chemical field [35]. It is important to mention here that all thermodynamic calculations were done in gas phase and they could not be used in solution.

## CONCLUSION

In the present work, we have calculated the geometric parameters, the vibrational frequencies, frontier orbital band gap, MESP surfaces, the non-linear optical properties and thermo dynamical properties of Pyridine and Pentachloropyridine (PCP) using DFT/B3LYP method. The calculated optimized structures of both molecules are planner. The frontier orbital gap in case of PCP (5.26323 eV) is found to be lower than Pyridine (6.09018 eV) which shows that PCP is more polarizable and soft molecule. A good agreement between experimental and calculated normal modes of vibrations has been observed.

## REFERENCES

- [1] T. Anderson, *J. Liebigs Ann. Chem.*, **1846**, 60, 86-103.
- [2] Pyridine And Pyridine Derivatives Vol 20; Kirk-Othmer Kirk-Othmer Encyclopedia of Chemical Technology (4th Edition).
- [3] M.J. Frisch, G.W. Trucks, H.B. Schlegel, G.E. Scuseria, M.A. Robb, J.R. Cheeseman, G. Scalmani, V. Barone, B. Mennucci, G.A. Petersson, H. Nakatsuji, M. Caricato, X. Li, H.P. Hratchian, A.F. Izmaylov, J. Bloino, G. Zheng, J.L. Sonnenberg, M. Hada, M. Ehara, K. Toyota, R. Fukuda, J. Hasegawa, M. Ishida, T. Nakajima, Y. Honda, O. Kitao, H. Nakai, T. Vreven, J.A. Montgomery Jr., J.E. Peralta, F. Ogliaro, M. Bearpark, J.J. Heyd, E. Brothers, K.N. Kudin, V.N. Staroverov, R. Kobayashi, J. Normand, K. Raghavachari, A. Rendell, J.C. Burant, S.S. Iyengar, J. Tomasi, M. Cossi, N. Rega, J.M. Millam, M. Klene, J.E. Knox, J.B. Cross, V. Bakken, C. Adamo, J. Jaramillo, R. Gomperts, R.E. Stratmann, O. Yazyev, A.J. Austin, R. Cammi, C. Pomelli, J.W. Ochterski, R.L. Martin, K. Morokuma, V.G. Zakrzewski, G.A. Voth, P. Salvador, J.J. Dannenberg, S. Dapprich, A.D. Daniels, Ö. Farkas, J.B. Foresman, J.V. Ortiz, J. Cioslowski, D.J. Fox, Gaussian 09, Revision A.1, Gaussian, Inc., Wallingford CT, 2009.
- [4] C. Lee, A.D. Yang, R.G. Parr, *Phys. Rev.*, **1988**, B 37, 785–789.
- [5] A.D. Becke, *J. Chem. Phys.*, **1993**, 98 1372–1377.
- [6] M. Karabacak, M. Kurt, M. Cinar, A. Coruh, *Mol. Phys.*, **2009**, 107, 253-264.
- [7] N.Sundaraganesan, S.Ilakiamani, H.Saleem, P.M.Wojciechowski, D. Michalska, *Spectrochim. Acta A*, **2005**, 61, 2995-3001.
- [8] A. Frisch, A.B. Nielson, A.J. Holder, GAUSS VIEW Users Manual, Gaussian Inc., Pittsburgh, PA, **2000**.
- [9] <http://webbook.nist.gov/chemistry/form-ser.html>, **2012**.
- [10] D.A. Kleinman, *Phys. Rev.*, **1962**, 126, 1977–1979.
- [11] J. Pipek, P.Z. Mezey, *J. Chem. Phys.*, **1989**, 90, 4916–4926.
- [12] A.D. Buckingham, *Adv. Chem. Phys.*, **1967**, 12, 107-142.
- [13] M. Bakiler, I.V. Maslov, S. Akyuz, *J. Mol. Struct.*, **1999**, 475, 83-92.
- [14] M. Bakiler, I.V. Maslov, S. Akyuz, *J. Mol. Struct.*, **1998**, 379, 482–483.
- [15] Fleming I., *Frontier Orbitals and Organic Chemical Reactions*, John Wiley and Sons, New York (**1976**)
- [16] Y.X. Sun, Q.L. Hao, W.X. Wei, Z.X. Yu, L.D. Lu, X. Wang, Y.S. Wang, *J. Mol. Struct.: Theochem*, **2009**, 904, 74–82.
- [17] C. Andraud, T. Brotin, C. Garcia, F. Pelle, P. Goldner, B. Bigot, A. Collet, *J. Am. Chem. Soc.*, **1994**, 116, 2094–2102.
- [18] V.M. Geskin, C. Lambert, J.L. Bredas, *J. Am. Chem. Soc.*, **2003**, 125, 15651–15658.
- [19] M. Nakano, H. Fujita, M. Takahata, K. Yamaguchi, *J. Am. Chem. Soc.*, **2002**, 124, 9648–9655.
- [20] D. Sajan, H. Joe, V.S. Jayakumar, J. Zaleski, *J. Mol. Struct.*, **2006**, 785, 43–53.
- [21] P.M. Anbarasana, M. K. Subramanian, P. Senthilkumar, C. Mohanasundaram, V. Ilangovan, N. Sundaraganesan, *J. Chem. Pharm. Res.*, **2011**, 3(1), 597-612
- [22] P. Singh, N. P. Singh and R. A. Yadav, *J. Chem. Pharm. Res.*, **2011**, 3(1), 737-755
- [23] R. Singh, M. Kumar, P. Singh and R A Yadav, *J. Chem. Pharm. Res.*, **2011**, 3(3), 25-37
- [24] P.M. Anbarasan, M. K. Subramanian, S. Manimegalai, K. Suguna, V. Ilangovan, N.Sundaraganesan, *J. Chem. Pharm. Res.*, **2011**, 3(3), 123-136.

- 
- [25] G. Fogarasi, P. Pulay, in: J.R. Durig (Ed.), *Vibrational Spectra and Structure*, Elsevier, Amsterdam, **1985**, 14, 125 (Chapter 3).
- [26] G. Fogarasi, X. Zhou, P.W. Taylor, P. Pulay, *J. Am. Chem. Soc.*, **1992**, 114, 8191-8201.
- [27] T.Sundius, *J.Mol. Spectrosc.*,**1980**, 82, 138-151.
- [28] T.Sundius, *J.Mol.Struct.*,**1990**, 218, 321-336.
- [29] T.Sundius, *Vib. Spectrosc.*,**2002**, 29, 89-95.
- [30] G. Varsanyi, *Assignments of Vibrational Spectra of 700 Benzene Derivatives*, Wiley, New York, **1974**.
- [31] R.A. Yadav, I.S. Singh, *Indian J. Pure Appl. Phys.*,**1985**, 23, 626-627.
- [32] N. Sundaraganesan, S. Illakiamani, C. Meganathan, B.D. Joshua, *Spectrochim.Acta A*,**2007**,67, 214–224.
- [33] J. Bevan Ott., J.Boerio-Goates, *Calculations from Statistical Thermodynamics*, Academic Press, **2000**.
- [34] D. Sajan, L. Josepha, N. Vijayan, M. Karabacak, *Spectrochim. Acta A*,**2011**, 81, 85-98.
- [35] R. Zhang, B. Dub, G. Sun, Y. Sun, *Sprctrochim. Acta A*,**2010**, 75, 1115-1124.